JVST B
Journal of Vacuum Science & Technology B

ARTICLE

avs.scitation.org/journal/jvb

Sol-gel synthesized indium tin oxide as a transparent conducting oxide with solution-processed black phosphorus for its integration into solar-cells

Cite as: J. Vac. Sci. Technol. B 38, 063203 (2020); doi: 10.1116/6.0000471
Submitted: 19 July 2020 · Accepted: 22 September 2020 ·
Published Online: 9 October 2020

Ravindra Mehta,[1] Misook Min,[1] and Anupama B. Kaul[1,2,a)]

AFFILIATIONS

[1]Department of Materials Science and Engineering; PACCAR Technology Institute, University of North Texas, Denton, Texas 76203
[2]Department of Electrical Engineering; University of North Texas, Denton, Texas 76203

[a)]**Electronic mail:** Anupama.kaul@unt.edu

ABSTRACT

In this work, indium tin oxide (ITO) thin films were synthesized using solgel processing with a mixture of $InCl_3$, methanol, and $SnCl_2$, where the solutions were spin coated onto glass substrates. The maximum transmittance of the ITO thin film in the visible region was found to be ~75% for films annealed at 650 °C, where plasma treatment of the substrate was found to aid in the large-area continuity and homogeneity over the glass substrates compared to films annealed at lower temperatures. Two-dimensional (2D), semiconducting black phosphorus (BP) dispersions were then prepared by liquid exfoliation, where the black phosphorus bulk crystals were finely ground inside a glove box and dissolved in *N*-cyclohexyl-2-pyrrolidone. Following further treatment, the BP solution dispersions were drop cast onto the transparent ITO thin films to form heterostructures toward transparent electronics and future solar cell applications. Direct electrical probing of the black phosphorus revealed that it was electrically conducting and the currents measured were large on the order of a few microampere at ~20 V. Raman and photoluminescence measurements on the black phosphorus revealed that the flakes ranged in thickness from few-layers up to bulk. Few-layer black phosphorus can be distinguished from the bulk through the red-shift of the A_g^1, B_g^2, and A_g^2 peaks for bulk black phosphorus flakes compared to the few-layers' black phosphorus flakes. Electrical measurements made in the heterostructure interfaces showed a higher magnitude of currents at the black phosphorus interface compared to the bare ITO film. The combined architecture of black phosphorus on ITO thin films shows promise in its use for transparent electronics, which can also serve as a stepping stone for future solar cell platforms.

I. INTRODUCTION

The integration of two-dimensional (2D) materials with transparent conductive oxides (TCOs) can lead to fully transparent electronics. Transition metal dichalcogenides (TMDs) are important 2D materials with interesting optoelectronic properties suitable for light emitting diodes (LEDs) and photovoltaics.[1] Transition metal dichalcogenides have attracted much attention due to their 2D layered structure, where a sheet of metal atoms is sandwiched between two sheets of chalcogens through a covalent interaction. Depending on the selection of the metal, these layered materials may exhibit superconducting, metallic, or semiconducting properties.[1,2] Moreover, the band structure of the semiconducting TMDCs, such as molybdenum disulfide (MoS_2), tungsten disulfide (WS_2), and tungsten diselenide (WSe_2), also shows a variation with thickness; for example, a transition of WSe_2 from the indirect gap (~1.3 eV) in the bulk form to direct gap (~1.6 eV) when in its monolayer (ML) form is evident merely as a result of quantum confinement due to band structure changes.[3]

More recently, semiconducting black phosphorus (BP), the most stable phosphorus allotrope, has been the focus of much activity over the past several years.[4] Black phosphorus consists of an orthorhombic crystal structure where the phosphorus atoms are stacked in hexagonal honeycomb layers with weak out-of-plane van der Waals bonding. The sp^3 hybridization between phosphorus

atoms in the plane results in a strong covalent interaction. Similar to TMDCs, the BP bandgap E_g is thickness dependent varying from ~0.3 eV for bulk to ~2 eV for the monolayer,[3] and contrary to TMDC's, where a direct E_g is only exhibited at one layer, in BP, a direct E_g is maintained at all thicknesses.[5]

Two-dimensional materials can be synthesized via bottom up approaches that include physical and chemical vapor deposition techniques or top-down approaches that involve mechanical or liquid exfoliation techniques. Liquid phase exfoliation offers unique advantages of low-cost, low temperature processing devoid of the need to work in a strictly controlled cleanroom environment, and the possibility for large-area device fabrication.[6] Liquid phase exfoliation of 2D materials is prominent for applications in composite materials, flexible electronics, and catalysis. The bulk crystal is grounded into powder and dissolved in the chemically active solvent and sonicated for a specific duration, which mechanically shears the crystal planes overcoming the weaker van der Waals bonds.[7]

At the same time, stretchable and printed electronics show vast potential for the use of 2D materials in a wide range of applications, such as energy storage, transparent electrodes, and ultrarapid transistors.[8] The unique properties of 2D materials serve as a potential to overcome some of the challenges with silicon for electronics and optoelectronic devices.[9] Many 2D materials offer promising carrier mobilities that provide the potential for realizing high-speed devices such as field-effect transistors.[10] For several device applications, such as solar cells, light emitting diodes, and field-effect transistors, a high work function metal contact is desired, where contact engineering has also been a significant focus for research activities.[11]

The minimal dangling bonds present at the surface of 2D crystalline materials result in superior interface quality to minimize trapped charges, which are critical for high-performance devices. For example, trapped charges at metal-semiconductor junctions often deteriorate device performance at such heterostructures.[12,13] Interestingly, it has also been shown that the bandgap in some 2D materials can be tuned by the application of an external electric field, and the bandgap in some of the TMDCs undergoes a transition from semiconducting to metallic.[14]

Two-dimensional materials can be synthesized via mechanical exfoliation, liquid exfoliation, or CVD growth. Transparent conductive oxides can serve as a good contact material for devices and 2D materials can be used as layers for ultrafast carrier transport.[15] Using monolayer MoS_2 as a hole transport material and zinc oxide as an electron transport layer enables us to achieve efficient, low-cost, and durable solar cells.[16] Black phosphorus is an interesting 2D material since it combines unique attributes of both TMDCs and graphene, i.e., it offers bandgap tunability and high mobility. It is a direct bandgap semiconductor regardless of the number of layers[17] with a unique puckered structure.[18] The 2D BP is a p-type semiconductor with a high hole mobility of 1000 cm^2/Vs at room temperature, where devices with high I_{on}/I_{off} ratios ~10^5 have been achieved in transistors.[19]

Transparent conductive oxides, such as indium tin oxide (ITO), can serve as a good contact material for devices, and 2D materials can be used as layers for ultrafast carrier transport.[15] ITO films generally provide increased adhesion to a wider variety of substrates, higher transmittance values, and higher conductivity compared to other transparent conductive oxides such as zinc oxide (ZnO) and aluminum doped zinc oxide (AZO).[20,21] The ITO is also more resistant to degradation when exposed to moisture compared to ZnO and AZO.[22] Physical vapor deposition is a common technique to deposit ITO thin films to achieve very high transmittance and low resistivity, however, a high vacuum requirement and the sophisticated process needed makes the fabrication very expensive. The use of a solution-based process eliminates these requirements and dramatically reduces the processing cost. A solgel based process can produce ITO thin films with low porosity and good optoelectronic properties.[23] Here, conduction occurs during the annealing step when the tin atoms substitute for the indium atoms, which creates oxygen vacancies and generates free electrons for conduction, making it an n-type semiconductor.[24]

In this work, we describe the synthesis of ITO and its integration with solution-processed 2D BP. For the ITO synthesis, the doping concentration of tin was maintained at 5 wt. %, below which there is not enough carrier concentration to generate enough free electrons for conduction and above which, increase in oxygen vacancies' scatters electrons.[23] Tin doped indium oxide solution has a shelf life of about two months, however, it is best to utilize the solution within a week after its preparation because gelation beyond one week will make it very viscous and it is difficult to achieve uniform films with controlled thickness.[25] The spin coating technique offers better control of thickness and uniformity compared to spray coating or dip coating, which also employ the solgel route.[26] The use of N-cyclohexyl-2-pyrrolidone (CHP) solvent for liquid exfoliation of BP increases its oxidation resistance by providing a solvation shell.[27] Since it is well known that BP is unstable at ambient atmospheres, thus, the solvation shell produced by CHP is effective in minimizing oxidation induced effects. Black phosphorus has been drop cast for these initial tests where the bottom contact should remain accessible for electrical probing which is why it is not spin cast. If BP is spin coated on ITO, then the entire ITO region will be covered with BP, making the ITO inaccessible as a bottom electrode for electrical probing.

The transparent conductive oxides can be electrically conducting while at the same time allowing light to enter the solar cell. Fore contacts must have n-type conductivity.[28] The motivation for using transparent conductive oxides with BP stems from the fact that this bilayer will lead to further developments for their use in future solar cell platforms. Since ITO is an n-type semiconductor commonly used as a front-end electrode for solar cells due to its ability to allow a large fraction of incoming light to be transmitted to the active layer, it also serves as a good electrical contact at the same time with low resistivity. The use of ITO electrodes for solar cell applications is, thus, the preferred choice since it increases efficiency by allowing more photocarriers to be generated given that a large fraction of the light is transmitted.[20,21]

II. MATERIALS AND METHODS

A. Preparation of ITO thin films

Tin doped indium oxide solution was synthesized by mixing 0.5 g of indium chloride in 25 ml methanol and 0.025 g of dihydrate tin chloride in 15 ml methanol. The precursors of the solution to prepare the films were mixed such that the ratio

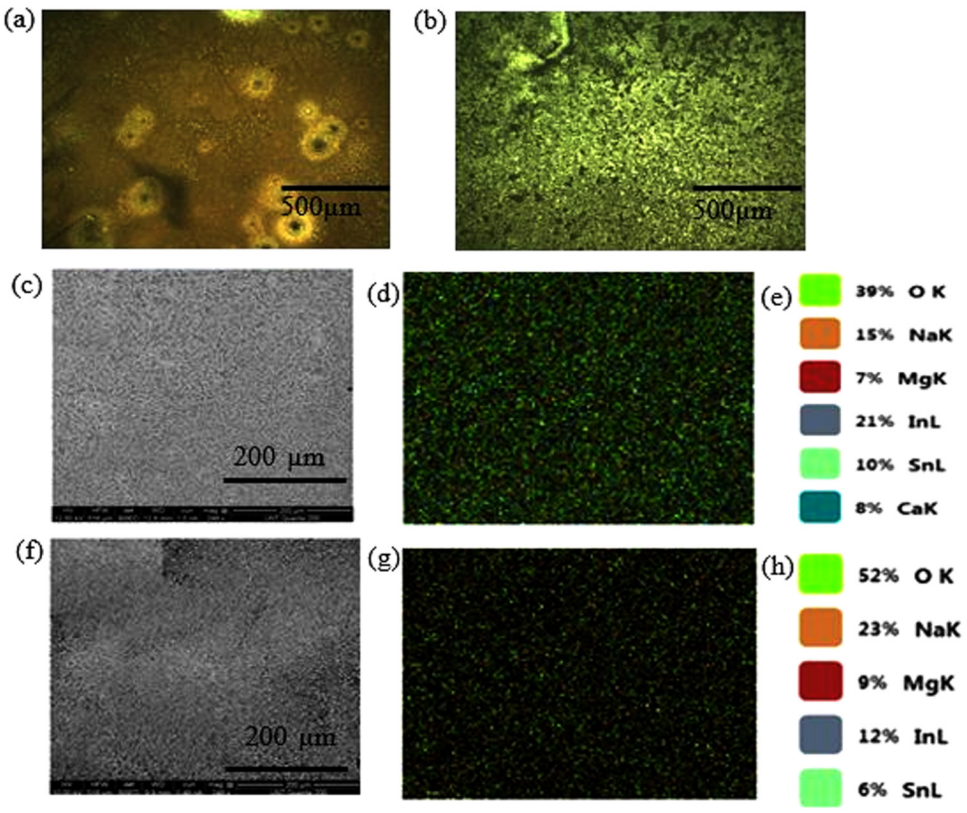

FIG. 1. Optical image of the ITO thin film deposited on (a) glass without plasma treatment showing the discontinuous film with cluster formation and (b) plasma-treated glass for 5 min showing a continuous film. Both samples were annealed at 550 °C. SEM micrograph, EDS map, and chemical composition of the ITO thin films annealed at 550 °C [(c)–(e)] and 650 °C [(f)–(h)], respectively, indicating the higher degree of oxidation and continuity for the films annealed at 650 °C. The images in (d) and (g) represent the areal map of the composition, and (e) and (h) correspond to the weight percentages for the two annealing temperatures used, respectively.

$\frac{\text{weight of tin}}{\text{weight of tin+weight of indium}} \times 100 \sim 5\%$. The two solutions were mixed and stirred at 60 °C for 2 h, few drops of hydrochloric acid were added for stabilization and the solution was left as it for about a week for gelation. The oxygen plasma treatment of the substrate helps improve the continuity of the film as the wettability of the glass increases. However, prior studies[29] have found that beyond 5 min of oxygen plasma treatment, the films smoothen out due to splitting hills. Thus, the glass substrates were plasma treated for 5 min in the present work. As shown in Fig. 1(a), the substrates processed without oxygen plasma-treatment results in a discontinuous ITO thin film with the formation of ITO clusters, while the substrates processed with oxygen plasma-treatment results in a continuous ITO thin film. The ITO coated glass substrates were then annealed at 550 °C and 650 °C in air. It was found from previous runs and the literature that the substrates annealed at these temperatures have better properties than the ones annealed at lower temperatures.[30] Temperatures greater than 650 °C were not used since the glass used cannot withstand such high temperatures before cracking and damage.

B. Preparation of the BP layer

Few-layered BP was liquid exfoliated on top of the ITO thin films annealed at 650 °C since a higher transmittance was obtained

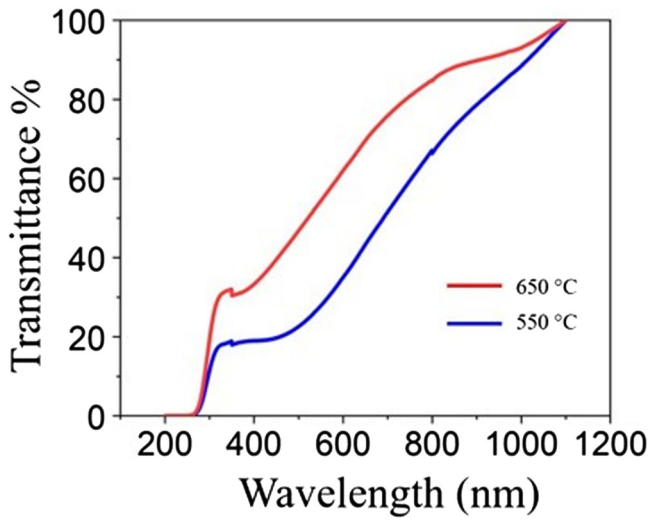

FIG. 2. Transmittance comparison of ITO thin films annealed at 550 °C (blue) and 650 °C (red) where the annealing time used was 30 min on a plasma-treated glass substrate indicating higher transmittance for the ITO thin film annealed at 650 °C.

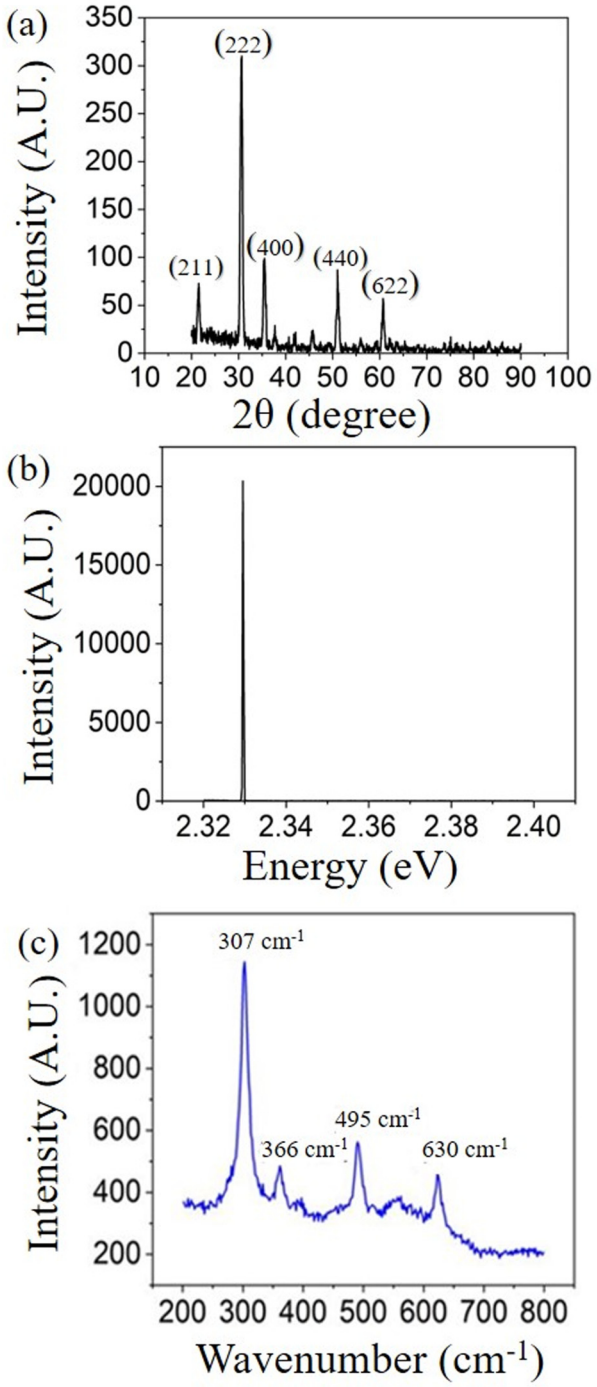

FIG. 3. (a) XRD spectra, (b) PL spectra, and (c) Raman spectra for the ITO thin film annealed at 650 °C for 30 min. The sharply defined peaks in the XRD spectra in (a), the well-defined bandgap tabulated to be ∼ 2.33 eV from the PL data in (b), and the signature Raman peaks in (c) suggestive of the cubic bixbyite crystal structure, indicate the good crystalline morphology and wide bandgap semiconducting character of our ITO thin films synthesized here.

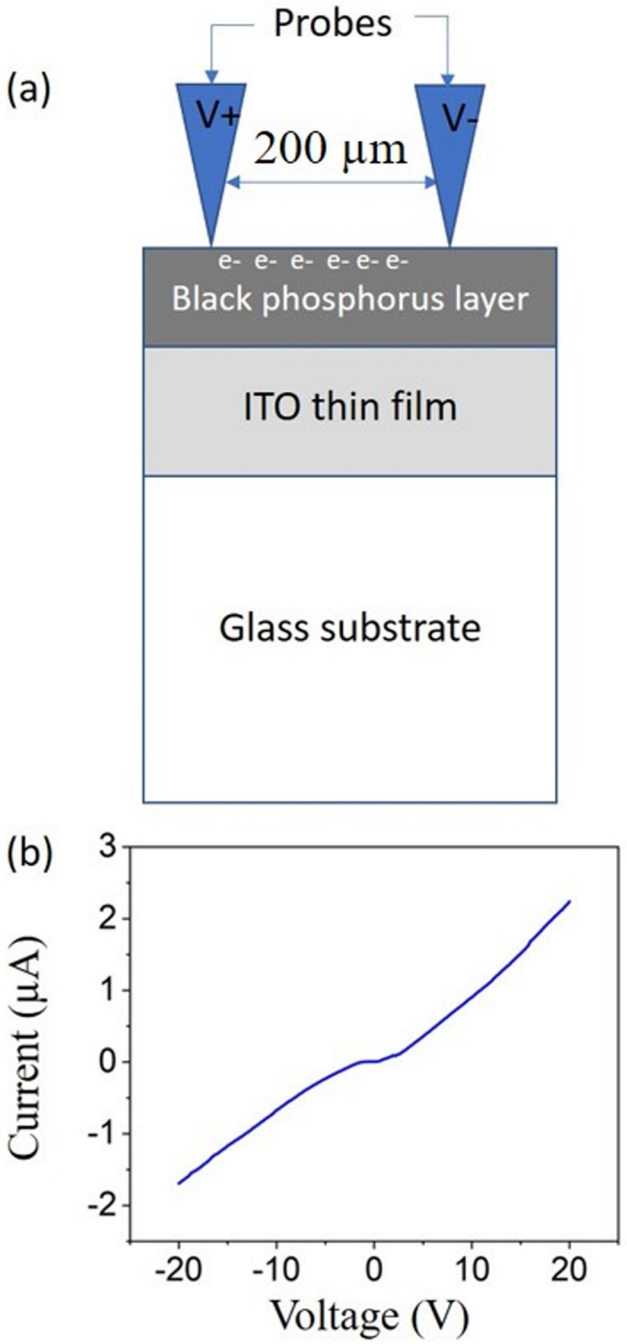

FIG. 4. (a) Schematic illustration to depict the electrical probing conducted on the black phosphorus layer residing on the ITO, where the two probes are spaced ∼200 μm apart. Here, the black phosphorus layer is liquid exfoliated on top of the solgel synthesized ITO thin film dispersed onto soda-lime glass. (b) *I*–*V* curve measured on liquid exfoliated black phosphorus layer on the ITO thin film, indicating black phosphorus is conducting in the orders of microamperes which is at least 10× higher than other reported work.

for those films annealed at the higher temperature. The preparation of BP crystal for solution processing started by first finely grinding it in a mortar and pestle inside the glove box where the oxygen and moisture levels were carefully controlled to be less than 0.1 ppm. 60 mg of BP powder was dissolved in 12 ml of *N*-cyclohexyl-2-pyrrolidone inside the conical tube in the glove box apparatus. Following this, the tube was sealed using Teflon tape/three layers parafilm, and the tube was placed inside the sonicator for 24 h at 30 °C. The water inside the sonicator was changed every 100 min since it would get heated up. The solution was drop cast on the ITO coated glass, and the sample was heated up to 70 °C for 30 min to evaporate the solvent followed by annealing at 250 °C for 2 h on a hot plate. The black phosphorus film coated on ITO deposited substrate was then placed inside the vacuum desiccator and removed only for the purpose of conducting material characterization or electrical measurements.

III. RESULTS AND DISCUSSIONS

A. Characterization of the ITO thin film

The films were characterized using a number of techniques such as profilometry for thickness determination, optical absorption spectroscopy for finding the transmittance as a function of wavelength, and Raman spectroscopy measurements to verify the chemical fingerprints of the ITO. The spin coating speed and time were optimized and the solution was spin coated at 1500 rpm for 30 s and the ramp rate was 500 rpm. Prior to spin coating, the glass substrates were cleaned using acetone, alcohol, and de-ionized water. The glass substrates were then plasma treated using an oxygen plasma at 60 standard cubic centimeters per minute and 298 mTorr. The ITO spin-coated substrates were then annealed at 550 and 650 °C in air.

As can be seen from the scanning electron microscope (SEM) image and energy dispersive spectroscopy (EDS) analysis in Figs. 1(c)–1(h), the ITO thin films spin coated and annealed at 550 and 650 °C appear to be largely continuous and homogeneous. From Figs. 1(e) and 1(h), the oxygen concentration of the film annealed at 650 °C is relatively higher than the oxygen concentration of the film annealed at 550 °C, which indicates that the films annealed at 650 °C are oxidized to a greater extent.

Transmittance measurement of the ITO coated glass substrates was performed using the CARY UV–VIS spectrophotometer. It can be seen from Fig. 2, the maximum transmittance in the visible region was determined to be ~51% for the film annealed at 550 °C and ~75% for the film annealed 650 °C, where the annealing time used was 30 min. The higher transmittance value for the ITO thin films annealed at 650 °C is likely to do with its more oxygen-rich composition, better continuity, and homogeneity, compared to the films annealed at 550 °C. The average thickness of the ITO thin films is around 150 ± 10 nm.

It is seen that the transmittance value of the ITO thin film is somewhat lower, however, the continuity obtained is much better compared to the non-plasma treated substrate, upon which the ITO was deposited, as can be seen from the comparative analysis of Figs. 1(a) and 1(b), respectively. The plasma treatment of the substrate prior to spin coating increases surface roughness, which

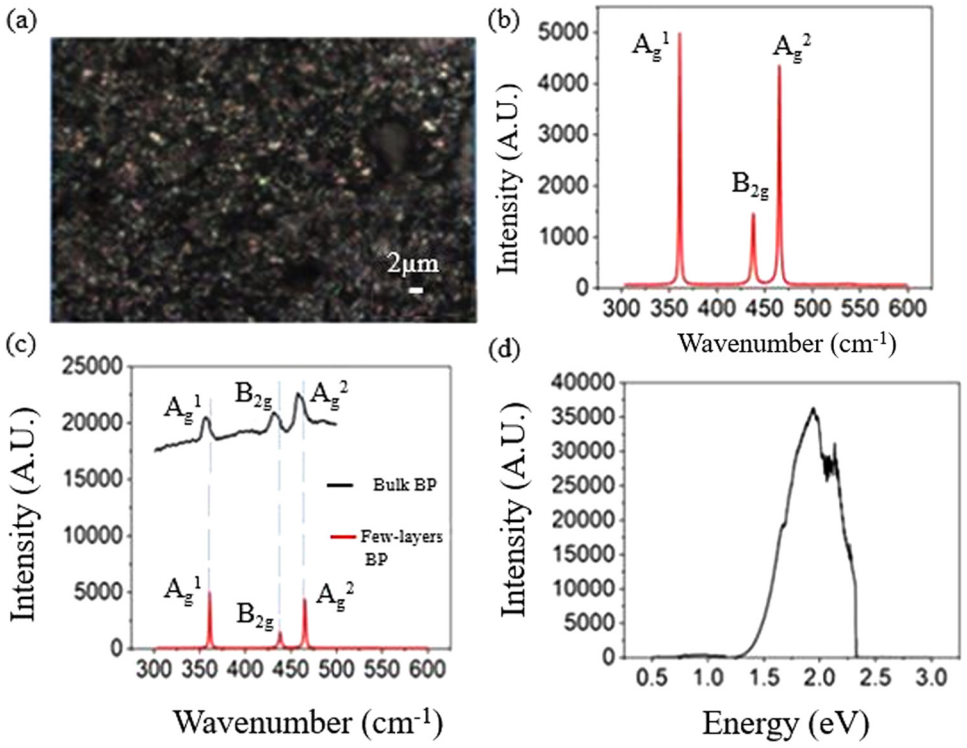

FIG. 5. (a) Optical image of the black phosphorus flake exfoliated on the ITO thin film annealed at 650 °C. (b) Raman spectra of the black phosphorus flake indicating few-layers' black phosphorus. (c) Raman shift indicating the red-shift in going from few-layer black phosphorus flakes to bulk. (d) PL spectra of the few-layers' black phosphorus flakes on top of the ITO thin film showing a bandgap of ~ 1.8 eV, which confirms the presence of few-layers of black phosphorus.

holds the films on to the substrate more firmly, thereby improving the uniformity, but the increased surface roughness also scatters light which, to some extent, reduces the transmittance of the ITO coated glass. The maximum transmittance of the ITO thin film reported by Dong *et al.*[31] is 85% on the non-plasma treated glass substrate where the ITO film appears to be discontinuous, compared to the current work where the maximum transmittance is 75% for our continuous ITO thin film deposited on a plasma treated glass substrate.

As can be seen from x-ray diffraction (XRD) data in Fig. 3(a), the ITO thin film is highly crystalline and the peaks are in alignment with data obtained in other studies.[31] The photoluminescence (PL) spectra for the ITO thin film annealed at 650 °C for 30 min in Fig. 3(b) shows a very sharp peak with a bandgap of 2.33 eV, which lies within the bandgap range of wide bandgap semiconductors. The Raman peaks gathered for the ITO thin film annealed at 650 °C in Fig. 3(c) show that these are characteristic peaks of the cubic bixbyite crystal structure. The sharp and well-defined peaks are attributes of the high-quality ITO thin films we have synthesized here.[32,33]

B. Characterization of black phosphorus flakes

Electrical characterization was performed using a micromanipulator 450PM-B probe stage equipped with an Agilent 4156A precision semiconductor parameter analyzer. The sample was then mounted on the probe stage to proceed with the dc *I–V* measurements. The schematic of the layered architecture with the BP integrated with ITO is shown in Fig. 4(a) where the two probes spaced ~200 μm apart are shown. The *I–V* data are then gathered for the liquid exfoliated black phosphorus on the ITO thin film that is illustrated in Fig. 4(b). The transport in the BP layer shows a current of ~1 μA at 10 V, and from the *I–V* characteristic, a nonohmic character at low voltages is evident, given BP's intrinsically p-type semiconducting nature.[34] The magnitude of current obtained for the BP flakes in this work is similar in magnitude compared to that reported by Seo *et al.*[35] where the BP flakes were also obtained using liquid exfoliation.

Raman spectroscopy was performed using a Horiba LabRAM HR Evolution Microscope. The optical image of the region where the Raman and photoluminescence spectra were gathered is shown in Fig. 5(a). The Raman spectra in Fig. 5(b) indicate a few-layered BP.[36] The Raman shift comparison for the bulk and few-layers' black phosphorus in Fig. 5(c) shows a red-shift by 4.549, 6.798, and 7.712 cm^{-1} for the A_g^1, B_g^2, and A_g^2 phonon modes, respectively, for the few-layers' BP relative to bulk which is slightly higher than the red-shift reported in other studies[36] where red-shift values were 2.1, 2, and 1.5 cm^{-1} for the A_g^1, B_g^2, and A_g^2 modes, respectively. The higher red-shift in this work is likely due to the effects of the underlying solgel processed ITO thin film. The bandgap of bulk BP is 0.3 eV, as has been verified previously.[37] The bandgap measured for the few-layered BP flake on top of the ITO thin film is shown by the photoluminescence spectra in Fig. 5(d), where the bandgap was measured to be ~1.8 eV.

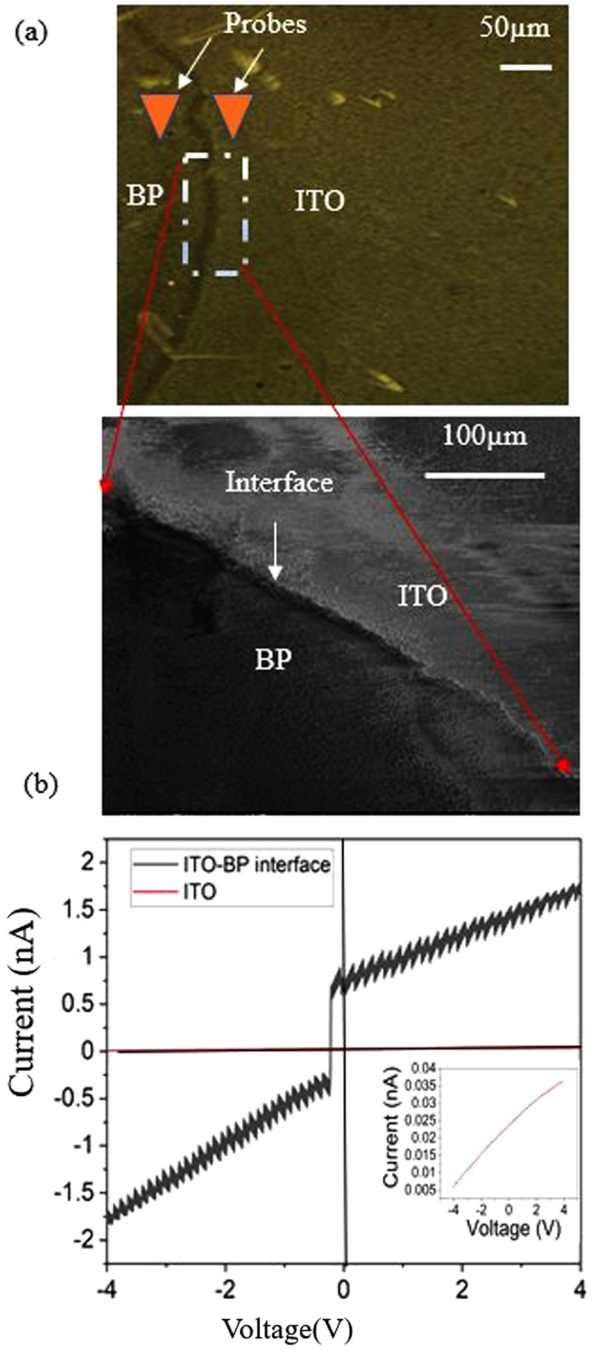

FIG. 6. (a) (Top) Optical micrograph of ITO–BP lateral interface showing the schematic of the probes landed across each side and, (bottom) the corresponding SEM image of the lateral junction which reveals the lateral junction length to be ~ 20 μm. (b) Electrical characterization of the ITO–BP interface, where there is a steep increase in current at low voltages of ~ –0.23 eV, after which point the current rises less rapidly. Here, the ITO was annealed at 650 °C for 30 min. The inset shows the *I–V* characteristic of the bare ITO film, where current levels are significantly lower, in the tens of pA range, compared to the ITO–BP heterointerface.

C. Characterization of the black phosphorus–ITO interface

ITO has been previously integrated with polystyrene doped black phosphorus to form a trilayer structure of ITO/BP@PS/ITO for its application in memristors.[38] Electrical characterization on these trilayer structures revealed a resistive switching mechanism where the current was measured by setting and resetting the read voltage. The trilayer architecture in this recent article by Zhou *et al.*[38] is clearly different from our bilayer ITO/BP junction architecture discussed in this work for which no prior published reports were found, to date. Besides the difference in device architecture, Zhou *et al.*[38] synthesized their ITO thin films using thermal evaporation, while in our current study, we have utilized a solution-based approach using solgel spin casting. Additionally, in our work, the BP was not intentionally doped, while polystyrene was used as an intentional dopant for black phosphorus in Zhou's study. The magnitude of the maximum current reported by Zhou *et al.* is 100 mA.[38] We have analyzed the interface of ITO and BP in more detail through imaging and electrical measurements via direct probing. Figure 6 (a, top) shows the optical micrograph of both the ITO and black phosphorus sides of the junction, and the schematic indicates the approximate region where the probes were landed on each side (left probe on the BP side and right probe on the ITO side) for the electrical measurements. Shown in Fig. 6(a, bottom) is the corresponding higher magnification scanning electron microscope (SEM) image of the lateral interface, and from this analysis, the lateral interface traversed a length of $\sim 20\,\mu$m. There is also likely interdiffusion of ITO occurring into the BP in the lateral interfacial region, possibly arising during the annealing step of the BP. At the interface, it is likely that the BP will scavenge oxygen from the ITO given its high propensity for O_2, and this will likely influence the electrical behavior at the junction. The bare ITO film was also direct probed to compare with the BP–ITO I–V characteristic, and the data are shown in Fig. 6(b) where the probe spacing was kept constant at $\sim 335\,\mu$m in both cases. The I–V characteristic obtained by directly probing ITO reveals that the current levels are suppressed compared to what was obtained by directly probing BP [Fig. 4(b)] or the BP–ITO interface. In the latter case, there is a steep increase in current at very low voltage, ~ -0.23 V as shown in Fig. 6(b), where there appears to be a rapid transfer of electrons from the n-type ITO toward the p-type BP once the barrier height is crossed. Once the majority of the electrons overcome the barrier, upon a further increase in voltage, the current increases at a reduced rate given the reduced slope of the I–V for higher voltages. More studies are needed to understand the nature of electrical transport in further detail through temperature-dependent measurements, which will be a topic for a future study.

IV. CONCLUSION

Tin doped indium oxide thin films were successfully synthesized using a solgel spin coating technique and characterized using optical absorption spectroscopy and photoluminescence. Continuity of the ITO thin film was improved by oxygen plasma treatment of the glass substrate upon which it was dispersed for 5 min, which improves wettability and surface free energy. The bandgap of ITO thin films reveals a wide bandgap consistent with prior findings. The maximum transmittance obtained was measured to be ~75% in the visible region. Black phosphorus flakes were successfully exfoliated and show current levels and conductivity of a significant magnitude, and the exfoliated flakes are both bulk as well as few layers, which were characterized by Raman and PL spectroscopy. The architecture utilized here in this study can be a stepping stone toward the feasibility of BP in future solar cell devices. The BP–ITO interface appears to enhance the electrical transport across the interface compared to the bare ITO films.

ACKNOWLEDGEMENTS

We thank the Office of Naval Research (ONR) (Grant No. ONR N00014-19-1-2142) that enabled us to pursue this work. A.B.K. is also grateful to the support received from the University of North Texas (UNT), along with the PACCAR Technology Institute and Endowed Professorship support.

REFERENCES

[1] A. K. Geim and I. V. Grigorieva, Nature **499**, 419 (2013).
[2] A. K. Geim and K. S. Novoselov, Nat. Mater. **6**, 183 (2007).
[3] J. Qiao, X. Kong, Z.-X. Hu, F. Yang, and W. Ji, Nat. Commun. **5**, 1 (2014).
[4] F. Xia, H. Wang, and Y. Jia, Nat. Commun. **5**, 1 (2014).
[5] L. Li, Y. Yu, G. J. Ye, Q. Ge, X. Ou, H. Wu, D. Feng, X. H. Chen, and Y. Zhang, Nat. Nanotechnol. **9**, 372 (2014).
[6] J. A. Desai, N. Adhikari, and A. B. Kaul, RSC Adv. **9**, 25805 (2019).
[7] S. Mazumder, J. A. Catalan, A. Delgado, H. Yamaguchi, C. N. Villarrubia, A. D. Mohite, and A. B. Kaul, Compos. Sci. Technol. **182**, 107687 (2019).
[8] J. A. Desai, S. Chugh, M. Michel, and A. B. Kaul, J. Mater. Sci. Mater. Electron. **30**, 12500 (2019).
[9] S. Chugh, N. Adhikari, J. H. Lee, D. Berman, L. Echegoyen, and A. B. Kaul, ACS Appl. Mater. Interfaces **11**, 24349 (2019).
[10] K. Jayanand, S. Chugh, N. Adhikari, M. Min, L. Echegoyen, and A. B. Kaul, J. Mater. Chem. C **8**, 3970 (2020).
[11] G. A. Saenz and A. B. Kaul, Surf. Coat. Technol. **382**, 125031 (2020).
[12] A. S. Bandyopadhyay, G. A. Saenz, and A. B. Kaul, Surf. Coat. Technol. **381**, 125084 (2020).
[13] A. S. Bandyopadhyay, N. Adhikari, and A. B. Kaul, Chem. Mater. **31**, 9861 (2019).
[14] A. B. Kaul, J. Mater. Res. **29**, 348 (2014).
[15] Z. Dai, Z. Wang, X. He, X.-X. Zhang, and H. N. Alshareef, Adv. Funct. Mater. **27**, 1703119 (2017).
[16] S. Kohnehpoushi, P. Nazari, B. A. Nejand, and M. Eskandari, Nanotechnology **29**, 205201 (2018).
[17] D. Li, J.-R. Xu, K. Ba, N. Xuan, M. Chen, Z. Sun, Y.-Z. Zhang, and Z. Zhang, 2D Mater. **4**, 031009 (2017).
[18] J.-W. Jiang and H. S. Park, J. Phys. D Appl. Phys. **47**, 385304 (2014).
[19] L. Li, M. Engel, D. B. Farmer, S.-J. Han, and H.-S. P. Wong, ACS Nano **10**, 4672 (2016).
[20] W.-J. Ho, M.-C. Huang, Y.-Y. Lee, Z.-F. Hou, and C.-J. Liao, Nanoscale Res. Lett. **9**, 1 (2014).
[21] K. Sakamoto, H. Kuwae, N. Kobayashi, A. Nobori, S. Shoji, and J. Mizuno, Sci. Rep. **8**, 2825 (2018).
[22] D. S. Ginley and J. D. Perkins, *Handbook of Transparent Conductors* (Springer, New York, 2010).

[23]Z. Chen, W. Li, R. Li, Y. Zhang, G. Xu, and H. Cheng, Langmuir **29**, 13836 (2013).
[24]M. Hjiri, F. Ghribi, and L. Mir, J. Sens. Transducers **27**, 198 (2014).
[25]S. R. Ramanan, Thin Solid Films **389**, 207 (2001).
[26]M. M.-H. Jafan, M.-R. Zamani-Meymian, R. Rahimi, and M. Rabbani, J. Nanostruct. Chem. **4**, 1 (2014).
[27]D. Hanlon *et al.*, Nat. Commun. **6**, 1 (2015).
[28]S. Ikhmayies, *Mediterranean Green Buildings and Renewable Energy* (Springer, Switzerland, 2019).
[29]B. W. N. H. Hemasiri, J.-K. Kim, and J.-M. Lee, Sci. Rep. **7**, 1 (2017).
[30]A. H. Ali, A. Shuhaimi, S. K. M. Bakhori, and H. Zainuriah, Adv. Mater. Res. **925**, 411 (2014).
[31]L. Dong, G. S. Zhu, H. R. Xu, X. P. Jiang, X. Y. Zhang, Y. Y. Zhao, D. L. Yan, L. Yuan, and A. B. Yu, J. Mater. Sci. Mater. Electron. **30**, 8047 (2019).
[32]M. Hijri, F. Ghribi, and L. Mir, Sens. Transducers **27**, 198 (2014).
[33]A. H. Sofi, M. A. Shah, and K. Asokan, J. Electron. Mater. **47**, 1344 (2017).
[34]P. D. Antunez, J. J. Buckley, and R. L. Brutchey, Nanoscale **3**, 2399 (2011).
[35]S. Seo *et al.*, Sci. Rep. **6**, 23736 (2016).
[36]H. B. Ribeiro, M. A. Pimenta, and C. J. De Matos, J. Raman Spectrosc. **49**, 76 (2017).
[37]B. Deng *et al.*, Nat. Commun. **8**, 14474 (2017).
[38]Y. Zhou *et al.*, ACS Appl. Mater. Interfaces **12**, 25108 (2020).